

NFPO: STABILIZED POLICY OPTIMIZATION OF NORMALIZING FLOW FOR ROBOTIC POLICY LEARNING

Diyuan Shi^{1,2,*}, Yiqi Tang^{2,*}, Zifeng Zhuang², Donglin Wang^{2,†}

¹Zhejiang University ²Westlake University *Equal Contribution †Corresponding Authors

ABSTRACT

Deep Reinforcement Learning (DRL) has experienced significant advancements in recent years and has been widely used in many fields. In DRL-based robotic policy learning, however, current *de facto* policy parameterization is still multivariate Gaussian (with diagonal covariance matrix), which lacks the ability to model multi-modal distribution. In this work, we explore the adoption of a modern network architecture, i.e. Normalizing Flow (NF) as the policy parameterization for its ability of multi-modal modeling, closed form of log probability and low computation and memory overhead. However, naively training NF in online Reinforcement Learning (RL) usually leads to training instability. We provide a detailed analysis for this phenomenon and successfully address it via simple but effective technique. With extensive experiments in multiple simulation environments, we show our method, NFPO could obtain robust and strong performance in widely used robotic learning tasks and successfully transfer into real-world robots.

1 INTRODUCTION

Deep Reinforcement Learning (DRL), as a machine learning field studying sequential decision making, has received tremendous research interest and advancements in recent years (Mnih et al., 2015; Ouyang et al., 2022; DeepSeek-AI et al., 2025). With reduced Sim-to-Real gap (Margolis et al., 2022c; Fu et al., 2022), nowadays the policies trained in parallel simulation environments by RL could be transferred with unprecedented easiness to real world robotic systems. This avoids the need to manually collect real data which is highly expensive and cumbersome, significantly speeding up the researches and developments. Through this way, many policies trained by DRL have been successfully deployed and enabled impressive accomplishments in generating smooth, autonomous motions on real-world bipedal, quadruped and humanoid robots (Li et al., 2023; Lee et al., 2020; Ze et al., 2025; Margolis et al., 2022b; Radosavovic et al., 2024; Zhang et al., 2025; Shao et al., 2025).

However, current *de facto* policy parameterization in DRL robotic policy learning is still multivariate Gaussian with diagonal covariance matrix which is known to have poor ability to model multi-modal distributions. This is in stark contrast to another paradigm, Supervised-Learning-Based robotic policy learning (a.k.a Behavior Cloning where a policy is trained to mimic pre-collected behavior dataset) where modern policy networks like Diffusion Policy (Chi et al., 2023; Liao et al., 2025) and Transformers (Brohan et al., 2023b;a) are in wide adoption.

While many recent works have studied the integration of diffusion-based policies into Online Reinforcement Learning paradigm, most of them are built on off-policy methods (like Soft Actor Critic (SAC) (Haarnoja et al., 2018)) for stronger sample efficiency. While in robotic learning, simulation environments offer massive samples with *trivial cost* and it’s 1) computation efficiency, 2) memory consumption and 3) robustness towards multiple simulator and reward function settings are of more importance. Under this setting, on-policy methods like Proximal Policy Optimization (PPO) (Schulman et al., 2017a;b) are more favored and have delivered countless successes. Unfortunately, it remains unclear how to integrate modern multi-modal-modeling networks into Policy Optimization’s paradigm, and train control policy purely from scratch¹. A table comparison between our method and related works could be found in Table 1.

¹There also exist methods that perform purely offline or offline-to-online finetuning of diffusion or Transformer policies via RL for robots. But we focus on from-scratch DRL learning where no dataset is present.

Table 1: Comparison of NFPO to related methods. Detailed explanations of how we choose ✓ or ✗ and the references are provided in Section A.1.

Algorithm	Multi-modality	On-policy	Memory & Computation	Real World Deployment
FastTD3	✗	✗	✗	✓
Meow	✓	✗	✓	✗
MaxEntDP	✓	✗	✗	✗
GenPO	✓	✓	✗	✗
FPO ^α	✓	✓	✓	✗
Ours (NFPO)	✓	✓	✓	✓

^α This work is finished concurrently to FPO. After that, a recent work, FPO++ (Yi et al., 2026) could be successfully deployed onto robotic platform.

In this work, we aim to bridge this gap by designing a new method which is 1) computation and memory efficient, 2) robust towards multiple simulator and reward function settings and 3) simple with few code changes to current training pipeline. We choose Normalizing Flow (NF) as it naturally fits all above requirements. However, naively combining NF with Policy Optimization would cause severe training and numerical instability. We provide detailed analysis and show how to address it with simple but effective techniques. In summary, our contributions are:

1. Aiming at robotic multi-modal policy learning, we integrate NF into PPO, analyze the reasons of its training instability and propose methods to address it.
2. We extensively test our method in multiple widely-used simulation environments (IsaacGym, Mujoco-playground and IsaacLab) and demonstrate our method (with the same set of configurations) could obtain competitive performance compared to state-of-the-art Gaussian PPO implementation.
3. We successfully transfer the policy trained with NFPO to real-world robots to show it could perform various tasks like locomotion and motion tracking.

2 RELATED WORKS

Deep Reinforcement Learning. DRL has experienced tremendous advancements in recent years. From on-policy methods like TRPO (Schulman et al., 2017a), PPO (Schulman et al., 2017b) to off-policy methods like DQN (Mnih et al., 2015), DDQN (van Hasselt et al., 2015), TD3 (Fujimoto et al., 2018) and SAC (Haarnoja et al., 2018), a main research direction is to improve the *sample-efficiency* which measures how many samples a method needs to achieve certain return, as humans could learn very efficiently with few interactions. By leveraging learnable dynamics and reward models, Model-based RL like Dreamer (Hafner et al., 2025) and TDMPC (Hansen et al., 2024) further increases the sample-efficiency compared to their model-free alternatives. Inspired by recent innovations in neural network architecture like Diffusion Model, Transformers and Normalizing Flows, another line of works targeting on combining these powerful networks into DRL’s framework has also emerged as in Chao et al. (2024); Ding et al. (2025); Dong et al. (2025). In this work, we try to integrate NFs into on-policy PPO’s pipeline as the latter is widely used in robotic policy learning.

Normalizing Flow. Normalizing Flow is a kind of generative models, featured by bijective mapping and closed calculation of log probability, compared to other generative methods like GAN (Goodfellow et al., 2014), Diffusion Models (Ho et al., 2020) and Score-based Models (Song et al., 2020). Since the early works like Dinh et al. (2015; 2017), NFs have also gained significant improvement. Especially in Zhai et al. (2025), the flexibility and generation quality of NFs have gained much improvement by using attention techniques. In DRL, the efficient and accurate calculation of log probability has made NFs an appealing policy parameterization and some works have explored the combination of NFs and DRL as in (Chao et al., 2024; Ghugare & Eysenbach, 2025). However, to the best of our knowledge, we are the first to integrate NFs into on-policy RL setting.

Robotic Policy Learning. Thanks to the rapid advancements of GPU-based parallel simulation environments and reduced Sim-to-Real gap (Kumar et al., 2021; Fu et al., 2022), Robotic Policy Learning has garnered great progress. From bipedal, quadruped robots with locomotion skills like parkour (Miki et al., 2022), fast running (Margolis et al., 2022a) to humanoid robots where teleoper-

ation (Ze et al., 2025; He et al., 2024) and motion tracking (Liao et al., 2025) have enabled dancing, kicking and somersault, many agile and stable behaviors have been learned by DRL pipeline. Alternatively, in Supervised-Learning-based robotic policy learning, modern network architecture like Transformers and Diffusion Models have shown great advantages for their expressiveness, like in Chi et al. (2023); Ren et al. (2024); Brohan et al. (2023a); Octo Model Team et al. (2024). In this work, we try to explore the integration of NFs as policy parameterizations in DRL paradigm.

3 BACKGROUND

Reinforcement Learning. Reinforcement Learning (RL) aims to solve sequential decision-making problem which is formulated as a Markovian Decision Process (MDP): $\mathcal{M} = \{\mathcal{S}, \mathcal{A}, \mathcal{R}, P, \gamma, \mathcal{S}_0\}$ where \mathcal{S} is the set of all *states*, \mathcal{A} is the set of all *actions*, $\mathcal{R} : (s_t, a_t) \rightarrow \mathbb{R}$ is the reward function that gives a scalar value for given state action pair, $P : s_{t+1} \sim P(s_t, a_t)$ is the transition model that gives the next state given current state action, γ is the discount factor and \mathcal{S}_0 is the distribution of initial states. RL is to find a policy function π that maximizes the expected return in \mathcal{M} :

$$\pi = \arg \max_{\pi \sim \Pi} \mathbb{E} \left[\sum_{t=0}^{\infty} \gamma^t \mathcal{R}(s_t, a_t) \right] \quad (1)$$

Proximal Policy Optimization. As a notable variant of on-policy RL, Proximal Policy Optimization (PPO) (Schulman et al., 2017b) performs policy optimization via advantage-based clip updates:

$$\pi_{\text{new}} = \arg \max_{\theta} \mathbb{E}_{a \sim \pi_{\text{old}}, s \sim P(s, a)} \left[\min(r(\theta) \tilde{A}(s, a), \text{clip}(r(\theta), 1 - \epsilon, 1 + \epsilon) \tilde{A}(s, a)) \right] \quad (2)$$

where $r(\theta) = \frac{\pi_{\theta}(a|s)}{\pi_{\text{old}}(a|s)}$ is the ratio of action likelihood and $\tilde{A}(s, a)$ is the estimated advantages (e.g., Generalized Advantage Estimation (GAE) as in Schulman et al. (2018)). As it requires log probability of action given state, the common policy parameterization is Gaussian with learnable mean and diagonal covariance matrix: $\pi(s) = \mathcal{N}(\mu_{\theta}(s), \text{diag}(\sigma_{\theta}(s)))$.

Normalizing Flow. Normalizing Flow (NF) is a bijective mapping with learnable components $f_{\theta} : \mathbb{R}^D \rightarrow \mathbb{R}^D$ between data distribution $p(x)$ and prior distribution $q(z)$. It’s designed such that the inverse f_{θ}^{-1} and the determinant of its Jacobian $|\frac{df_{\theta}(x)}{dx}|$ is in closed form and could be efficiently computed. The prior distribution is chosen as simple ones like Normal distribution. Then the data density could be expressed as:

$$p(x) = q(f_{\theta}(x)) \left| \frac{df_{\theta}(x)}{dx} \right| \quad (3)$$

Then we could use Maximum Likelihood Estimation (MLE) based training objectives $\theta = \arg \max_{\theta} \mathbb{E}_x [\log q(f_{\theta}(x)) + \log |\frac{df_{\theta}(x)}{dx}|]$, and perform *sampling* via $z \sim q(z)$; $x = f_{\theta}^{-1}(z)$ and *inference* via $x \sim p(x)$; $z = f_{\theta}(x)$.

RealNVP. An important NF variant is RealNVP (Dinh et al., 2017) with *coupling layers*:

$$f_{\theta}(x)_d = x_d \quad (4)$$

$$f_{\theta}(x)_{\setminus d} = x_{\setminus d} \odot \exp(s_{\theta}(x_d)) + t_{\theta}(x_d) \quad (5)$$

where d is a set containing certain indexes, $\setminus d = \{i | 1 \leq i \leq D, i \in \mathbb{N}^+ \setminus d\}$ is a set containing remaining indexes, \odot is element-wise production and s_{θ}, t_{θ} are 2 neural network from $\mathbb{R}^{|d|}$ to $\mathbb{R}^{|D-d|}$. From above definition, the Jacobian is: $|\frac{df_{\theta}(x)}{dx}| = \exp[\sum s(x_d)]$. Following the original work, we employ alternating odd-even strategy to partition the index set in which 3 or more stacked layers is needed to allow each dimension in x to influence each other.

4 METHOD

With above definition of PPO and NFs, we could build an optimization pipeline where NFs are used as policy parameterizations instead of Gaussian. Thanks to its closed form of log probability, the changes mainly involve a new calculation of $\pi(a|s)$ and sampling from prior distribution to generate action samples. All other components and formulas could be reused. However, a naive applying of above methods would likely result in training instability, for the following reasons:

1. **Overfitting.** Expressive multi-modality policies are prone to overfitting than Gaussian-based counterparts. As the modeling ability increases, the network could find a cheap optimization strategy that assigns high log-probability to all points with positive advantages and vice versa. An illustrative diagram is in Figure 1.
2. **Exponential values.** the $\exp(s_\theta(x_d))$ used in RealNVP applies exponential transformations on the output of neural networks. This further increases the tendency of overfitting as simply increase $s_\theta(x_d)$ would increase the training objective significantly.
3. **Unbounded Output.** Unlike Gaussian whose log-probability is roughly bounded (so long as the standard deviation is not infinitesimal), neural network’s output could be unbounded and lead to numerical instability values.

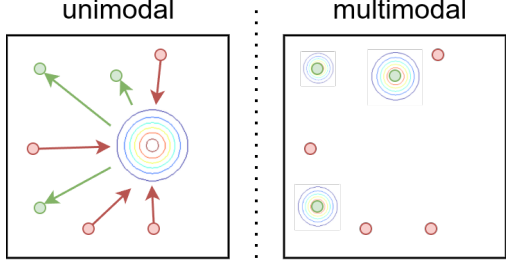


Figure 1: Illustrative diagram of multi-modal overfitting. Green samples are those whose probability needs increase while red samples need decrease. In left figure, the unimodal model cannot fit all these training signals but in the right figure a multimodal model overfits.

To further illustrate above phenomenon, we perform an experiment using UnitreeRLGym’s g1 environment. Specifically, we build a 4-layered RealNVP as policy parameterization and integrate it into PPO’s training pipeline, the training result is in Figure 2 under name of `s_none`.

From the result, we find the performance of `s_none` increases in the first and middle stage of training. However, the determinant of its Jacobian keeps increasing to very large values then it triggers numeric instability and training crashes.

Solution. As observed above, the training instability of NFs under Policy Optimization is mainly caused by the exponential transformation of unbounded output of $s_\theta(x)$. A simple yet effective technique is to ‘normalize’ the $s_\theta(x)$ output to make it in proper range. In this section, we test various methods for normalizing $s(x)$ to make it in bounded range. In details, we test 1) `no_s` where we omit $s(x)$ and only use $t(x)$. This is reported in Chao et al. (2024)

to have sufficient expressiveness in online RL setting, 2) `s_clip` where a $\text{clip}(s_\theta(x), -l, l)$ is applied with a hyperparameter l , 3) `s_tanh` where we use $l \times \tanh(s_\theta(x))$ and 4) `s_asymmetric` which is reported in Andrade (2024) as an advanced ‘normalizing’ technique. We train all of these methods (with $l = 0.5$) with PPO in Unitree RL Gym’s g1 environment, and the result is in Figure 2.

From the result, we find `s_clip` and `s_tanh` are 2 most effective ‘normalizing’ methods and both `no_s` and `s_none` obtains insufficient performance. While `s_asymmetric` could obtain performance increase in the ending of training, the determinant of it is still in high scale. Finally, we choose `s_tanh` for its simplicity and robustness (in Section 5.1 we compare `s_tanh` and `s_clip` in experiments and provide an analysis over why tanh may be better than clip in Section A.2).

Finally, we could build a stabilized PPO-NF method which we name as NFPO (for brevity, the conditioned state s is omitted):

$$\begin{aligned} \pi_{\text{new}} &= \arg \max_{\theta} \mathbb{E} \left[\min(r(\theta) \tilde{A}(s, a), \text{clip}(r(\theta), 1 - \epsilon, 1 + \epsilon) \tilde{A}(s, a)) \right] \\ \log \pi(a) &= \log q(f_{\theta}(a)) + \sum_j \log \left| \frac{df_{\theta_j}(a)}{da} \right| \\ f_{\theta_j}(a)_{d_j} &= a_{d_j} \\ f_{\theta_j}(a)_{\setminus d_j} &= a_{\setminus d_j} \odot \exp(l \tanh(s_{\theta_j}(a_{d_j}))) + t_{\theta_j}(a_{d_j}) \end{aligned} \quad (6)$$

where j represents the j th coupling layer. A pseudo-code of NFPO is presented in Section A.8.

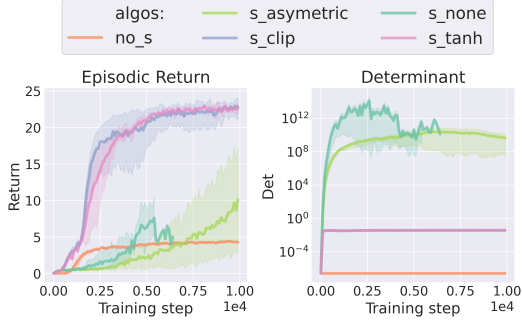


Figure 2: Training NFs in Unitree Gym’s g1. The experiment is in 3 seeds with 95% confidence interval. `s_none` early stopped due to training instability, `s_clip` and `s_tanh` overlaps in determinant plot.

5 EXPERIMENTS

In this section, we conduct experiments to answer several questions regarding NFPO’s properties: 1) How do various factors influence NFPO’s performance? 2) How is NFPO’s performance compared to state-of-the-art (SOTA) PPO implementations? 3) Does NFPO learn multi-modal behaviors? 4) How is NFPO compared to other multi-modal policy learning methods? 5) Could NFPO’s policy transfer to real-world robotic platforms? We conduct experiments in 2 widely used simulator: 1) Unitree RL Gym (URG) which is based on Nvidia IsaacGym (Makoviychuk et al., 2021) and is the official platform for training locomotion policies on Unitree’s robots (g1, h1 and go2); 2) Mujoco Playground (MJP) (Zakka et al., 2025) which uses MJX as the underlying parallel simulation.

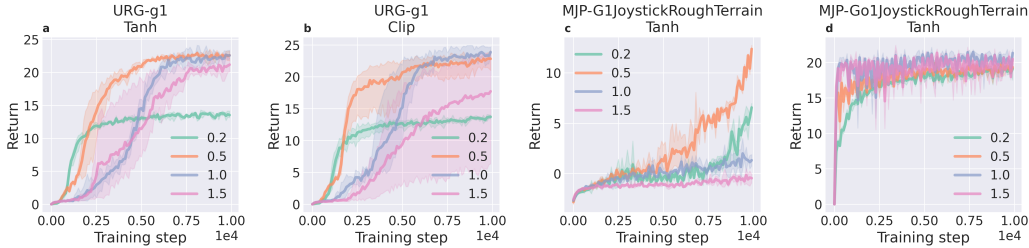


Figure 3: Studies in various factors. Experiments are in 3 seeds with 95% confidence interval.

5.1 Q1: HOW DO VARIOUS FACTORS INFLUENCE NFPO’S PERFORMANCE?

Our first experiment is to explore how various factors influence the NFPO’s performance. As we have observed, the ‘normalizing’ technique is very important in stabilizing the training of NFs, we hence choose several related factors: 1) the hyperparameter l , 2) tanh vs clip normalization, 3) an entropy term that is used in PPO to prevent mode collapsing and 4) adding certain level of noise to actions during training then remove it in sampling phase, similar to Zhai et al. (2025).

We firstly investigate the influence of ‘normalization’ techniques between clip and tanh in Figure 3 (subfigures a and b): Generally speaking, both clip and tanh could obtain strong performance given proper l values. However, tanh tends to be more robust towards l than clip hence is chosen in our implementation.

Then we check the influence of l on tanh by looking at subfigures a, c and d in Figure 3. In simpler environments like Go1JoystickRoughTerrain, various l values could bring similar performance. But in challenging tasks like g1 and G1JoyStickRoughTerrain, proper value of l plays a very important role in learning performance. From the results, we find 0.5 is a good default value that fits various tasks.

Another important component in PPO is its entropy loss which could help exploration and prevent the methods from collapsing in local optimum. While NFPO is a multi-modal policy, we test if entropy term still helps its learning. By looking at results in Figure 4 (subfigures a, c and e), we could find adding entropy performance difference and could even slow down the learning speed in G1JoyStickRoughTerrain.

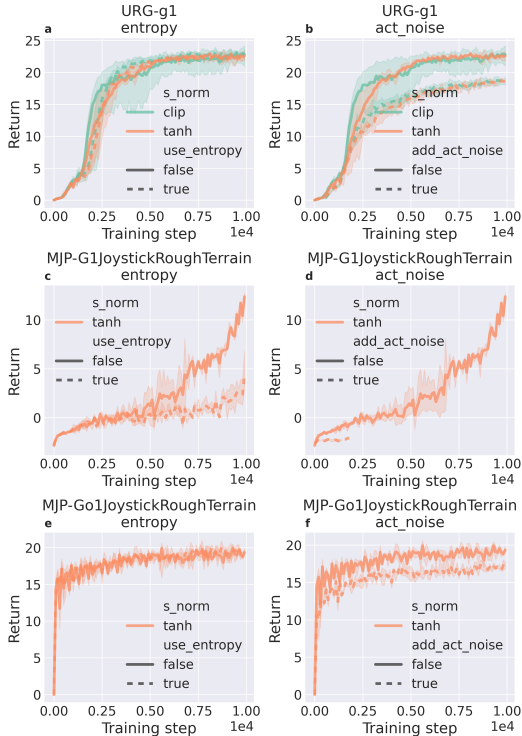


Figure 4: Studies in various factors. Experiments are in 3 seeds with 95% confidence interval.

Finally, as reported in Zhai et al. (2025), a critical technique to increase the image generation quality of NFs is to add Gaussian noise to training samples and remove this during generation, which is also observed in Ghugare & Eysenbach (2025). While our online RL settings have offered massive amount of continuous samples that could potentially reduce the need to ‘dequantize’ as in their dataset-based settings, we still test if adding this training noise and remove it during action sampling could help us further improve the performance. The results are in Figure 4 (subfigures **b**, **d** and **f**). Different from their settings, we find adding action noise would only decrease the RL performance in our tasks. Especially in some challenging environment like G1JoyStickRoughTerrain, it triggers training instability and early stops training at roughly 25% of total steps.

With above knowledge, we finally design our NFPO as a 4-layer RealNVP network with tanh transformations, remove entropy loss and use $l = 0.5$. **We use this configurations in all following experiments, replace Gaussian policy with it and find this obtains competitive performance without further tuning on other hyperparameters..**

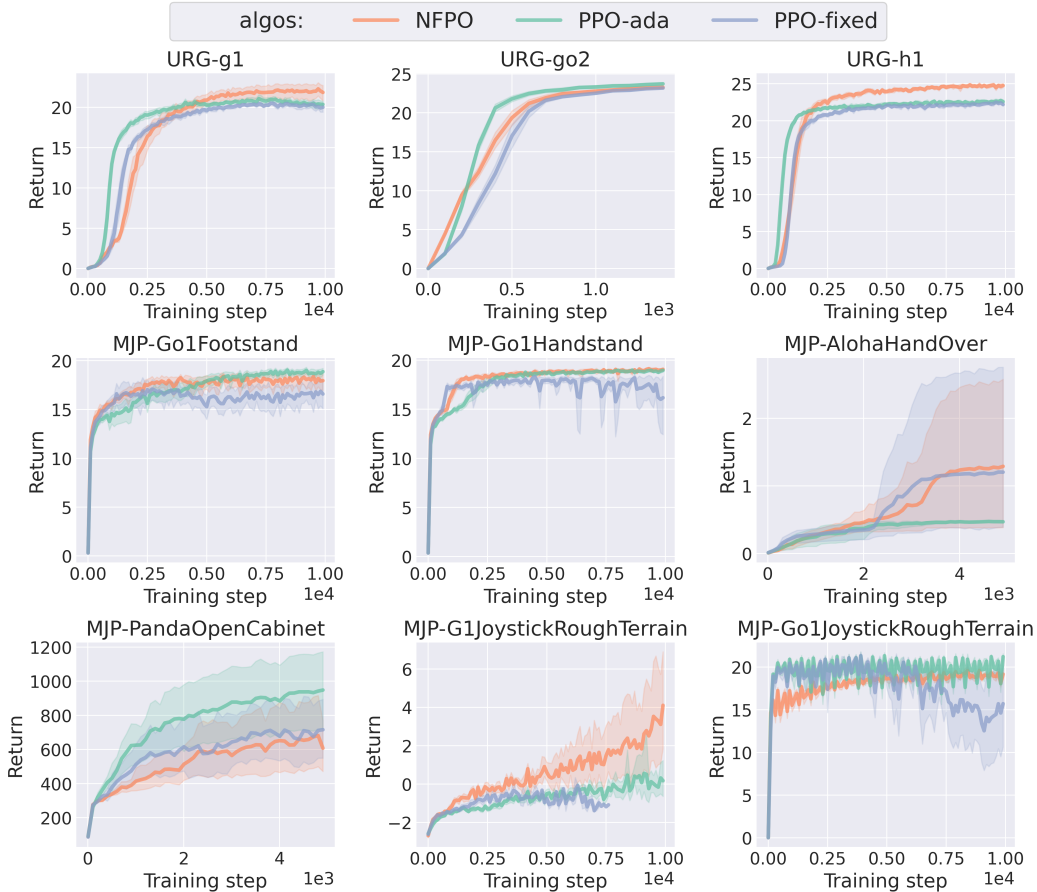


Figure 5: Learning curves of various methods on representative robotic tasks. The experiments are in 10 seeds. The errorbars are 95% confidence interval.

5.2 Q2: HOW IS NFPO’S PERFORMANCE COMPARED TO SOTA PPO IMPLEMENTATIONS?

In this section, we compare NFPO’s performance against RSL-RL (Schwarke et al., 2025)’s PPO implementation, the latter is current SOTA method that widely used in real-world oriented policy learning in countless Robotics works. We compare NFPO to 2 variants of PPO: 1) PPO-adaptive where the learning rate is dynamically scheduled for faster convergence and 2) PPO-fixed where the learning rate scheduler is disabled and is the default setting in Mujoco playground. The experiments are run in 10 seeds and shown in Figure 5. For a fair comparison, we have aligned the actor network

size of PPO and NFPO and most other components (e.g., value network) and hyperparameters (e.g., learning rate) are shared. The result is in Figure 5. We run 4096 parallel environments for unitree rl gym and 2048 for mujoco Playground.

From the result, we observe NFPO could achieve competitive or stronger performance compared to PPO baselines. Specifically, in high-dimensional control tasks like g1-joystick, h1-joystick and G1JoyStickRoughTerrain, our NFPO could achieve stronger convergence performance, thanks to its multi-modal modeling ability. On Go1JoystickRoughTerrain, NFPO’s performance fluctuates in less extent, reflecting it’s better to adapt to complex terrains. For simpler tasks like go2-joystick, NFPO still obtains similar performance against PPO. Finally, in manipulation tasks like AlohaHandOver and PandaOpenCabinet where exploration plays a more important part, the three tested methods exhibit complicated result with no one to be the best, indicating careful tuning is needed in these tasks. As for computation efficiency, on Unitree gym’s g1 environment, we observed a roughly 19% increase of wall-clock time in NFPO with details in Section A.10. For tasks in mujoco playground, we provide a video of NFPO’s policies in simulation in supplemental materials.

5.3 Q3: DOES NFPO LEARN MULTI-MODAL BEHAVIORS?

In this section, we test if NFPO could learn multi-modal behaviors given proper reward functions. Following works in FPO (McAllister et al., 2025), we use the gridworld example to demonstrate the difference in generated behaviors between NFPO and PPO. In gridworld environment, the agent is spawned in the grey cells and take continuous actions to move around. If it hits the green region, a positive reward would be granted otherwise the reward is 0.

The result is shown in Figure 6. The upper 2 figures depict the actions each policy would take in certain position and the lower 2 figures depict the generated 100 trajectories from the same starting point of each method. In this sparse reward setting, we could find NFPO tends to generate diverse actions that lead to various trajectories towards green region while PPO only takes the shortest way and doesn’t exhibit multi-modal behaviors.

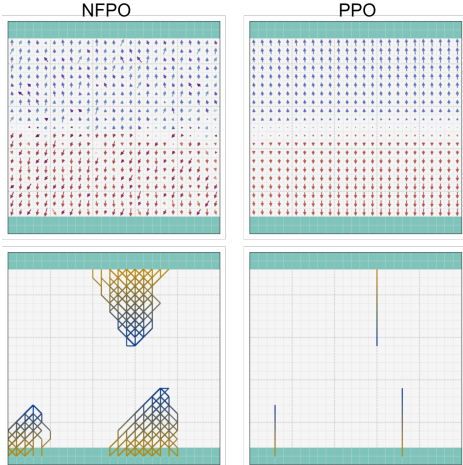


Figure 6: Difference in generated trajectory of NFPO and PPO in gridworld.

Besides, we also train NFPO and PPO in Isaac-Reach-UR10-v0 environment in IsaacLab (Mittal et al., 2023). Specifically, we design a sparse-reward variant of UR10 reaching where the arm would gain a positive reward when reaching to the given target position. After training both PPO and NFPO to convergence, we fix the initial state and target, then run both PPO and NFPO for 100 rollouts, and plot their trajectories in Figure 7 where ‘o’ marks the initial position (in xyz world frame) of end effector and ‘x’ marks the end position. We also attach the videos captured in IsaacLab’s simulation environment to better visualize the behavior difference between NFPO and PPO in supplemental materials.

From the result, we could find NFPO generates diverse trajectories while PPO only runs in rather fixed trajectories.

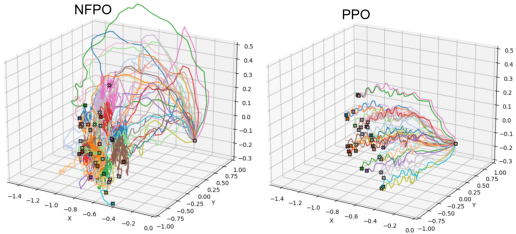


Figure 7: Difference in generated trajectories of NFPO and PPO in UR10 Reaching.

5.4 Q4: HOW IS NFPO COMPARED TO OTHER MULTI-MODAL POLICY LEARNING METHODS?

In this section, we try to compare NFPO against several related works that also employ multi-modal policy parameterizations in onlnt RL setting. However, as also illustrated in Table 1, not all methods hold equal fitness and potentials to be used in robotic policy learning. Specifically, there are 2 lines of works that deserve a discussion and comparison:

1. On-policy diffusion-model-based methods like GenPO (Ding et al., 2025) and FPO (McAllister et al., 2025). The difference between NFPO to these methods mainly locate in the difference between diffusion-based method and normalizing flows: In NFs, we have closed-form, easily-calculated log probability that could be directly chained to PPO’s training objective. While for diffusion models, various approximation methods need to be used and incur memory and computation overhead. As GenPO doesn’t release their source code and is hungry in memory and computation resources, we compare against FPO in this genre of methods.
2. Off-policy normalizing-flows-based methods like Meow (Chao et al., 2024) and Ghugare & Eysenbach (2025). The difference between NFPO to these methods mainly locate in the training paradigm of PPO to off-policy methods: Off-policy methods usually have a larger replay buffer and better sample-efficiency but fall short of computation and memory efficiency as also studied in Seo et al. (2025). In this line of work, we compare against Meow as Ghugare & Eysenbach (2025) doesn’t directly study conventional online RL settings.

As for other off-policy diffusion-based methods like MaxEntDP (Dong et al., 2025), QVPO (Ding et al., 2024) and QSM (Psenka et al., 2024), both their off-policy setting and approximation of log probability makes it non-trivial to integrate into normal training pipelines like IsaacGym and Mujoco Playground hence are omitted here.

In Figure 8, we present the training curves of Meow in Unitree RL gym’s g1 and go2 environment. In Meow, it has a novel design where no explicit policy network exists. Rather, it uses value function Q to parameterize the policy but this conflicts with the common asymmetric setting in robotic tasks where the value network and actor network have different observation dimensions and we have to feed actor observations (without privileged information) to its Q and V functions. Besides, we adjust its off-policy replay buffer’s dimension to (N_e, N_r, \dots) where the first dimension is the number of environments (4096 or 2048), the second dimension is its original buffer length (1.5e4). Following FastTD3, we also increased the batch size per each update while all other settings are either from their original implementation or the same to PPO and NFPO (details are in Section A.5). Under this setting, it costs roughly 50GB GPU memory for training on 4096 unitree gym’s g1 environment.

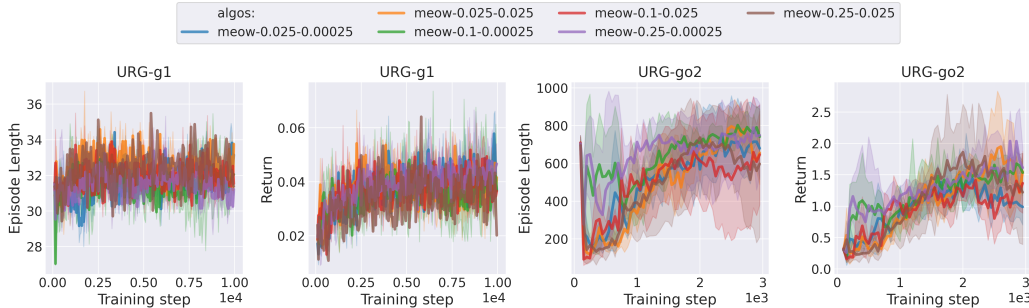


Figure 8: Learning curves of Meow and NFPO in 2 environments of Unitree RL Gym. Legend is meow-alpha-polyak where alpha and polyak are 2 tuned hyperparameters.

From the result, unfortunately, Meow doesn’t exhibit meaningful performance in g1 and go2 environments. In g1, both the episode length and episodic return stay in low values while in go2, episode length achieves high values in some phase, indicating Meow’s maximum-entropy learning framework could incentivize the exploration in some extent. However, the episodic return stays in low values and do not indicate a successful learning.

Table 2: NFPO and FPO’s accomplished tasks in Mujoco playground.

Task	FPO	NFPO
AlohaHandOver	✓	✗
G1JoystickRoughTerrain	✗	✓
Go1Footstand	✗	✓
Go1Handstand	✓	✓
Go1JoystickRoughTerrain	✗	✗
PandaOpenCabinet	✗	✓
PandaPickCube	✗	✓
Total	2	5

For FPO, we use their original codebase, and run the FPO’s training with their default hyperparameters on 7 mujoco playground’s tasks sim-

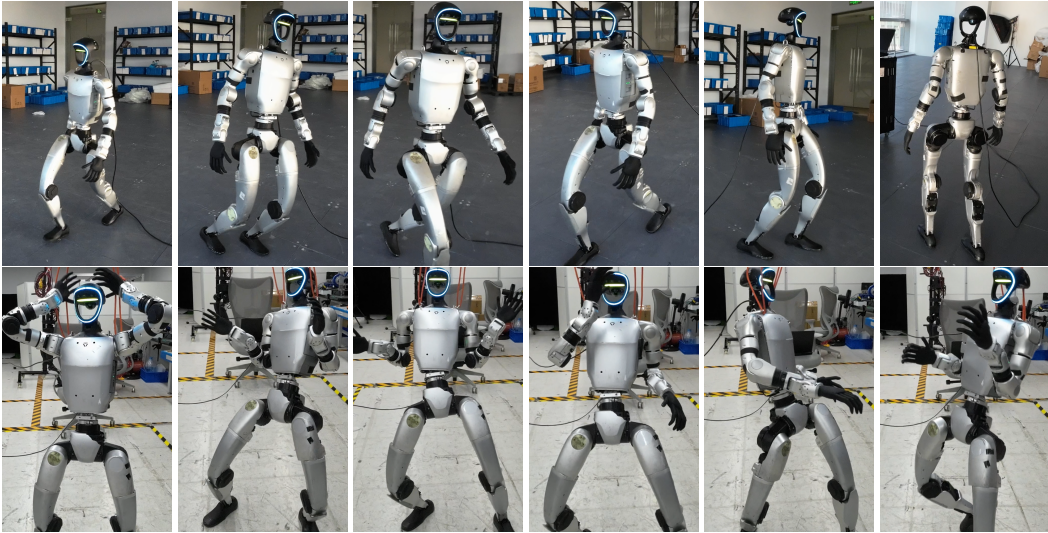


Figure 9: Snapshots of real world deployment video.

ilar to what we used in Figure 5. Then we visualize the learned policies in official mujoco playground’s codebase to see if they could successfully perform the tasks and show results in Table 2. For FPO, 2 out of 7 policies could show meaningful behaviors in simulation. And NFPO could perform 5 out of 7. Videos of both NFPO and FPO could be found in supplemental materials.

Integrating modern multi-modal policy into common robotic learning tasks is not a straightforward work, as the robotic tasks feature learning stability and memory and computation efficiency more than traditional RL tasks. And the purpose of this experiment is to showcase the learning stability and robustness of NFPO for which we use *a same set of configuration* across multiple simulation environments and tasks. It’s also important to note this experiment doesn’t mean FPO and Meow *won’t work in robotic policy learning*. Actually, with proper hyperparameter tuning and training adjustment, it’s likely for these methods to obtain improved performance, as in Seo et al. (2025).

5.5 Q5: COULD NFPO’S POLICY TRANSFER TO REAL-WORLD ROBOTIC PLATFORMS?

In this section, we transfer the policies trained by NFPO onto real-world robotic platform. In details, we choose Unitree RL Lab (Unitree Robotics, 2025) for training a joystick locomotion policy of and BeyondMimic (Liao et al., 2025) to train a dancing policy via motion-tracking. The robot is Unitree’s g1 and we use the common hierarchical structure where a high-level RL policy (trained by NFPO) outputs action target then a low-level PD controller outputs joint torque accordingly. The high-level policy runs in 50Hz and the low level PD controller runs in 200Hz. The video of real world deployment is in supplemental materials and a series of the video clips is provided in Figure 9. Similar to Chao et al. (2024), we have found deterministic version of NFPO could generate stable and smooth real world motions than its stochastic counterpart (A discussion is provided in Section A.6). From the results, we could find the policy trained in NFPO could successfully perform stable and agile 29-DoF whole-body control on unitree’s G1 robot.

6 CONCLUSION

In this work, aiming to unlock DRL-based multi-modal robotic policy learning, we explore the integration of Normalizing Flows to online Policy Optimization framework and have successfully built NFPO which is a stable method and could transfer to real-world robotic tasks.

In future works, we aim to further explore the benefits of NFPO to robotic policy learning, for example how to take advantages of its efficient calculation of log probability for interpretation and optimization of neural network based robotic policy.

REFERENCES

- Daniel Andrade. Stable Training of Normalizing Flows for High-dimensional Variational Inference. (arXiv:2402.16408), February 2024. doi: 10.48550/arXiv.2402.16408.
- Anthony Brohan, Noah Brown, Justice Carbajal, Yevgen Chebotar, Xi Chen, Krzysztof Choromanski, Tianli Ding, Danny Driess, Avinava Dubey, Chelsea Finn, Pete Florence, Chuyuan Fu, Montse Gonzalez Arenas, Keerthana Gopalakrishnan, Kehang Han, Karol Hausman, Alexander Herzog, Jasmine Hsu, Brian Ichter, Alex Irpan, Nikhil Joshi, Ryan Julian, Dmitry Kalashnikov, Yuheng Kuang, Isabel Leal, Lisa Lee, Tsang-Wei Edward Lee, Sergey Levine, Yao Lu, Henryk Michalewski, Igor Mordatch, Karl Pertsch, Kanishka Rao, Krista Reymann, Michael Ryoo, Grecia Salazar, Pannag Sanketi, Pierre Sermanet, Jaspiar Singh, Anikait Singh, Radu Soricut, Huong Tran, Vincent Vanhoucke, Quan Vuong, Ayzaan Wahid, Stefan Welker, Paul Wohlhart, Jialin Wu, Fei Xia, Ted Xiao, Peng Xu, Sichun Xu, Tianhe Yu, and Brianna Zitkovich. RT-2: Vision-Language-Action Models Transfer Web Knowledge to Robotic Control, July 2023a.
- Anthony Brohan, Noah Brown, Justice Carbajal, Yevgen Chebotar, Joseph Dabis, Chelsea Finn, Keerthana Gopalakrishnan, Karol Hausman, Alex Herzog, Jasmine Hsu, Julian Ibarz, Brian Ichter, Alex Irpan, Tomas Jackson, Sally Jesmonth, Nikhil J. Joshi, Ryan Julian, Dmitry Kalashnikov, Yuheng Kuang, Isabel Leal, Kuang-Huei Lee, Sergey Levine, Yao Lu, Utsav Malla, Deeksha Manjunath, Igor Mordatch, Ofir Nachum, Carolina Parada, Jodilyn Peralta, Emily Perez, Karl Pertsch, Jornell Quiambao, Kanishka Rao, Michael Ryoo, Grecia Salazar, Pannag Sanketi, Kevin Sayed, Jaspiar Singh, Sumedh Sontakke, Austin Stone, Clayton Tan, Huong Tran, Vincent Vanhoucke, Steve Vega, Quan Vuong, Fei Xia, Ted Xiao, Peng Xu, Sichun Xu, Tianhe Yu, and Brianna Zitkovich. RT-1: Robotics Transformer for Real-World Control at Scale, August 2023b.
- Chen-Hao Chao, Chien Feng, Wei-Fang Sun, Cheng-Kuang Lee, Simon See, and Chun-Yi Lee. Maximum Entropy Reinforcement Learning via Energy-Based Normalizing Flow. (arXiv:2405.13629), May 2024. doi: 10.48550/arXiv.2405.13629.
- Cheng Chi, Siyuan Feng, Yilun Du, Zhenjia Xu, Eric Cousineau, Benjamin Burchfiel, and Shuran Song. Diffusion Policy: Visuomotor Policy Learning via Action Diffusion. In *Proceedings of Robotics: Science and Systems (RSS)*, 2023.
- DeepSeek-AI, Daya Guo, Dejian Yang, Haowei Zhang, Junxiao Song, Ruoyu Zhang, Runxin Xu, Qihao Zhu, Shirong Ma, Peiyi Wang, Xiao Bi, Xiaokang Zhang, Xingkai Yu, Yu Wu, Z. F. Wu, Zhibin Gou, Zhihong Shao, Zhuoshu Li, Ziyi Gao, Aixin Liu, Bing Xue, Bingxuan Wang, Bochao Wu, Bei Feng, Chengda Lu, Chenggang Zhao, Chengqi Deng, Chenyu Zhang, Chong Ruan, Damai Dai, Deli Chen, Dongjie Ji, Erhang Li, Fangyun Lin, Fucong Dai, Fuli Luo, Guangbo Hao, Guanting Chen, Guowei Li, H. Zhang, Han Bao, Hanwei Xu, Haocheng Wang, Honghui Ding, Huajian Xin, Huazuo Gao, Hui Qu, Hui Li, Jianzhong Guo, Jiashi Li, Jiawei Wang, Jingchang Chen, Jingyang Yuan, Junjie Qiu, Junlong Li, J. L. Cai, Jiaqi Ni, Jian Liang, Jin Chen, Kai Dong, Kai Hu, Kaige Gao, Kang Guan, Kexin Huang, Kuai Yu, Lean Wang, Lecong Zhang, Liang Zhao, Litong Wang, Liyue Zhang, Lei Xu, Leyi Xia, Mingchuan Zhang, Minghua Zhang, Minghui Tang, Meng Li, Miaojun Wang, Mingming Li, Ning Tian, Panpan Huang, Peng Zhang, Qiancheng Wang, Qinyu Chen, Qiushi Du, Ruiqi Ge, Ruisong Zhang, Ruizhe Pan, Runji Wang, R. J. Chen, R. L. Jin, Ruyi Chen, Shanghao Lu, Shangyan Zhou, Shanhuang Chen, Shengfeng Ye, Shiyu Wang, Shuiping Yu, Shunfeng Zhou, Shuting Pan, S. S. Li, Shuang Zhou, Shaoqing Wu, Shengfeng Ye, Tao Yun, Tian Pei, Tianyu Sun, T. Wang, Wangding Zeng, Wanjin Zhao, Wen Liu, Wenfeng Liang, Wenjun Gao, Wenqin Yu, Wentao Zhang, W. L. Xiao, Wei An, Xiaodong Liu, Xiaohan Wang, Xiaokang Chen, Xiaotao Nie, Xin Cheng, Xin Liu, Xin Xie, Xingchao Liu, Xinyu Yang, Xinyuan Li, Xuecheng Su, Xuheng Lin, X. Q. Li, Xiangyue Jin, Xiaojin Shen, Xiaosha Chen, Xiaowen Sun, Xiaoxiang Wang, Xinnan Song, Xinyi Zhou, Xianzu Wang, Xinxia Shan, Y. K. Li, Y. Q. Wang, Y. X. Wei, Yang Zhang, Yanhong Xu, Yao Li, Yao Zhao, Yaofeng Sun, Yaohui Wang, Yi Yu, Yichao Zhang, Yifan Shi, Yiliang Xiong, Ying He, Yishi Piao, Yisong Wang, Yixuan Tan, Yiyang Ma, Yiyuan Liu, Yongqiang Guo, Yuan Ou, Yudian Wang, Yue Gong, Yuheng Zou, Yujia He, Yunfan Xiong, Yuxiang Luo, Yuxiang You, Yuxuan Liu, Yuyang Zhou, Y. X. Zhu, Yanhong Xu, Yanping Huang, Yaohui Li, Yi Zheng, Yuchen Zhu, Yunxian Ma, Ying Tang, Yukun Zha, Yuting Yan, Z. Z. Ren, Zehui Ren, Zhangli Sha, Zhe Fu, Zhean Xu, Zhenda Xie, Zhengyan Zhang, Zhewen Hao, Zhicheng Ma, Zhigang Yan, Zhiyu Wu, Zihui Gu, Zijia Zhu, Zijun Liu, Zilin Li, Ziwei Xie, Ziyang Song, Zizheng Pan, Zhen Huang, Zhipeng Xu, Zhongyu

- Zhang, and Zhen Zhang. DeepSeek-R1: Incentivizing Reasoning Capability in LLMs via Reinforcement Learning. (arXiv:2501.12948), January 2025. doi: 10.48550/arXiv.2501.12948.
- Shutong Ding, Ke Hu, Zhenhao Zhang, Kan Ren, Weinan Zhang, Jingyi Yu, Jingya Wang, and Ye Shi. Diffusion-based Reinforcement Learning via Q-weighted Variational Policy Optimization. (arXiv:2405.16173), May 2024. doi: 10.48550/arXiv.2405.16173.
- Shutong Ding, Ke Hu, Shan Zhong, Haoyang Luo, Weinan Zhang, Jingya Wang, Jun Wang, and Ye Shi. GenPO: Generative Diffusion Models Meet On-Policy Reinforcement Learning. (arXiv:2505.18763), May 2025. doi: 10.48550/arXiv.2505.18763.
- Laurent Dinh, David Krueger, and Yoshua Bengio. NICE: Non-linear Independent Components Estimation. (arXiv:1410.8516), April 2015. doi: 10.48550/arXiv.1410.8516.
- Laurent Dinh, Jascha Sohl-Dickstein, and Samy Bengio. Density estimation using Real NVP. (arXiv:1605.08803), February 2017. doi: 10.48550/arXiv.1605.08803.
- Xiaoyi Dong, Jian Cheng, and Xi Sheryl Zhang. Maximum Entropy Reinforcement Learning with Diffusion Policy. (arXiv:2502.11612), June 2025. doi: 10.48550/arXiv.2502.11612.
- Zipeng Fu, Xuxin Cheng, and Deepak Pathak. Deep Whole-Body Control: Learning a Unified Policy for Manipulation and Locomotion. (arXiv:2210.10044), October 2022. doi: 10.48550/arXiv.2210.10044.
- Scott Fujimoto, Herke van Hoof, and David Meger. Addressing Function Approximation Error in Actor-Critic Methods, October 2018.
- Raj Ghugare and Benjamin Eysenbach. Normalizing Flows are Capable Models for RL. <https://arxiv.org/abs/2505.23527v3>, May 2025.
- Ian J. Goodfellow, Jean Pouget-Abadie, Mehdi Mirza, Bing Xu, David Warde-Farley, Sherjil Ozair, Aaron Courville, and Yoshua Bengio. Generative Adversarial Networks. (arXiv:1406.2661), June 2014. doi: 10.48550/arXiv.1406.2661.
- Tuomas Haarnoja, Aurick Zhou, Pieter Abbeel, and Sergey Levine. Soft Actor-Critic: Off-Policy Maximum Entropy Deep Reinforcement Learning with a Stochastic Actor. (arXiv:1801.01290), August 2018. doi: 10.48550/arXiv.1801.01290.
- Danijar Hafner, Jurgis Pasukonis, Jimmy Ba, and Timothy Lillicrap. Mastering diverse control tasks through world models. *Nature*, pp. 1–7, April 2025. ISSN 1476-4687. doi: 10.1038/s41586-025-08744-2.
- Nicklas Hansen, Hao Su, and Xiaolong Wang. TD-MPC2: Scalable, Robust World Models for Continuous Control. (arXiv:2310.16828), March 2024. doi: 10.48550/arXiv.2310.16828.
- Tairan He, Zhengyi Luo, Xialin He, Wenli Xiao, Chong Zhang, Weinan Zhang, Kris Kitani, Changliu Liu, and Guanya Shi. OmniH2O: Universal and Dexterous Human-to-Humanoid Whole-Body Teleoperation and Learning. (arXiv:2406.08858), June 2024. doi: 10.48550/arXiv.2406.08858.
- Jonathan Ho, Ajay Jain, and Pieter Abbeel. Denoising Diffusion Probabilistic Models. (arXiv:2006.11239), December 2020. doi: 10.48550/arXiv.2006.11239.
- Shengyi Huang, Rousslan Fernand Julien Dossa, Chang Ye, Jeff Braga, Dipam Chakraborty, Kinan Mehta, and João G.M. Araújo. CleanRL: High-quality single-file implementations of deep reinforcement learning algorithms. *Journal of Machine Learning Research*, 23(274):1–18, 2022.
- Polina Kirichenko, Pavel Izmailov, and Andrew Gordon Wilson. Why Normalizing Flows Fail to Detect Out-of-Distribution Data. (arXiv:2006.08545), June 2020. doi: 10.48550/arXiv.2006.08545.
- Ashish Kumar, Zipeng Fu, Deepak Pathak, and Jitendra Malik. RMA: Rapid Motor Adaptation for Legged Robots. (arXiv:2107.04034), July 2021. doi: 10.48550/arXiv.2107.04034.

- Joonho Lee, Jemin Hwangbo, Lorenz Wellhausen, Vladlen Koltun, and Marco Hutter. Learning Quadrupedal Locomotion over Challenging Terrain. *Science Robotics*, 5(47):eabc5986, October 2020. ISSN 2470-9476. doi: 10.1126/scirobotics.abc5986.
- Zhongyu Li, Xue Bin Peng, Pieter Abbeel, Sergey Levine, Glen Berseth, and Koushil Sreenath. Robust and Versatile Bipedal Jumping Control through Reinforcement Learning. (arXiv:2302.09450), May 2023. doi: 10.48550/arXiv.2302.09450.
- Qiayuan Liao, Takara E. Truong, Xiaoyu Huang, Guy Tevet, Koushil Sreenath, and C. Karen Liu. BeyondMimic: From Motion Tracking to Versatile Humanoid Control via Guided Diffusion. (arXiv:2508.08241), August 2025. doi: 10.48550/arXiv.2508.08241.
- Viktor Makovychuk, Lukasz Wawrzyniak, Yunrong Guo, Michelle Lu, Kier Storey, Miles Macklin, David Hoeller, Nikita Rudin, Arthur Allshire, Ankur Handa, and Gavriel State. Isaac Gym: High Performance GPU Based Physics Simulation For Robot Learning. In *Thirty-Fifth Conference on Neural Information Processing Systems Datasets and Benchmarks Track (Round 2)*, August 2021.
- Gabriel Margolis, Ge Yang, Kartik Paigwar, Tao Chen, and Pulkit Agrawal. Rapid Locomotion via Reinforcement Learning. In *Robotics: Science and Systems*, 2022a.
- Gabriel B. Margolis, Ge Yang, Kartik Paigwar, Tao Chen, and Pulkit Agrawal. Rapid Locomotion via Reinforcement Learning. (arXiv:2205.02824), May 2022b. doi: 10.48550/arXiv.2205.02824.
- Gabriel B. Margolis, Ge Yang, Kartik Paigwar, Tao Chen, and Pulkit Agrawal. Rapid Locomotion via Reinforcement Learning. (arXiv:2205.02824), May 2022c. doi: 10.48550/arXiv.2205.02824.
- David McAllister, Songwei Ge, Brent Yi, Chung Min Kim, Ethan Weber, Hongsuk Choi, Haiwen Feng, and Angjoo Kanazawa. Flow Matching Policy Gradients. (arXiv:2507.21053), July 2025. doi: 10.48550/arXiv.2507.21053.
- Takahiro Miki, Joonho Lee, Jemin Hwangbo, Lorenz Wellhausen, Vladlen Koltun, and Marco Hutter. Learning robust perceptive locomotion for quadrupedal robots in the wild. *Science Robotics*, 7(62):eabk2822, 2022. doi: 10.1126/scirobotics.abk2822.
- Mayank Mittal, Calvin Yu, Qinxi Yu, Jingzhou Liu, Nikita Rudin, David Hoeller, Jia Lin Yuan, Ritvik Singh, Yunrong Guo, Hammad Mazhar, Ajay Mandlekar, Buck Babich, Gavriel State, Marco Hutter, and Animesh Garg. Orbit: A unified simulation framework for interactive robot learning environments. *IEEE Robotics and Automation Letters*, 8(6):3740–3747, 2023. doi: 10.1109/LRA.2023.3270034.
- Volodymyr Mnih, Koray Kavukcuoglu, David Silver, Andrei A. Rusu, Joel Veness, Marc G. Belle-mare, Alex Graves, Martin Riedmiller, Andreas K. Fidjeland, Georg Ostrovski, Stig Petersen, Charles Beattie, Amir Sadik, Ioannis Antonoglou, Helen King, Dhharshan Kumaran, Daan Wierstra, Shane Legg, and Demis Hassabis. Human-level control through deep reinforcement learning. *Nature*, 518(7540):529–533, February 2015. ISSN 1476-4687. doi: 10.1038/nature14236.
- Octo Model Team, Dibya Ghosh, Homer Walke, Karl Pertsch, Kevin Black, Oier Mees, Sudeep Dasari, Joey Hejna, Charles Xu, Jianlan Luo, Tobias Kreiman, You Liang Tan, Lawrence Yunliang Chen, Pannag Sanketi, Quan Vuong, Ted Xiao, Dorsa Sadigh, Chelsea Finn, and Sergey Levine. Octo: An open-source generalist robot policy. In *Proceedings of Robotics: Science and Systems*, Delft, Netherlands, 2024.
- Long Ouyang, Jeffrey Wu, Xu Jiang, Diogo Almeida, Carroll Wainwright, Pamela Mishkin, Chong Zhang, Sandhini Agarwal, Katarina Slama, Alex Ray, et al. Training language models to follow instructions with human feedback. *Advances in neural information processing systems*, 35: 27730–27744, 2022.
- Michael Psenka, Alejandro Escontrela, Pieter Abbeel, and Yi Ma. Learning a Diffusion Model Policy from Rewards via Q-Score Matching. (arXiv:2312.11752), July 2024. doi: 10.48550/arXiv.2312.11752.
- Ilija Radosavovic, Tete Xiao, Bike Zhang, Trevor Darrell, Jitendra Malik, and Koushil Sreenath. Real-world humanoid locomotion with reinforcement learning. *Science Robotics*, 9(89):eadi9579, 2024. doi: 10.1126/scirobotics.adi9579.

- Allen Z. Ren, Justin Lidard, Lars L. Ankile, Anthony Simeonov, Pulkit Agrawal, Anirudha Majumdar, Benjamin Burchfiel, Hongkai Dai, and Max Simchowitz. Diffusion Policy Policy Optimization. (arXiv:2409.00588), September 2024. doi: 10.48550/arXiv.2409.00588.
- John Schulman, Sergey Levine, Philipp Moritz, Michael I. Jordan, and Pieter Abbeel. Trust Region Policy Optimization. (arXiv:1502.05477), April 2017a. doi: 10.48550/arXiv.1502.05477.
- John Schulman, Filip Wolski, Prafulla Dhariwal, Alec Radford, and Oleg Klimov. Proximal policy optimization algorithms. *arXiv preprint arXiv:1707.06347*, 2017b.
- John Schulman, Philipp Moritz, Sergey Levine, Michael Jordan, and Pieter Abbeel. High-Dimensional Continuous Control Using Generalized Advantage Estimation. (arXiv:1506.02438), October 2018. doi: 10.48550/arXiv.1506.02438.
- Clemens Schwarke, Mayank Mittal, Nikita Rudin, David Hoeller, and Marco Hutter. RSL-RL: A learning library for robotics research. *arXiv preprint arXiv:2509.10771*, 2025.
- Younggyo Seo, Carmelo Sferrazza, Haoran Geng, Michal Nauman, Zhao-Heng Yin, and Pieter Abbeel. FastTD3: Simple, Fast, and Capable Reinforcement Learning for Humanoid Control. <https://arxiv.org/abs/2505.22642v3>, May 2025.
- Yiyang Shao, Xiaoyu Huang, Bike Zhang, Qiayuan Liao, Yuman Gao, Yufeng Chi, Zhongyu Li, Sophia Shao, and Koushil Sreenath. LangWBC: Language-directed Humanoid Whole-Body Control via End-to-end Learning. <https://arxiv.org/abs/2504.21738v1>, April 2025.
- Yang Song, Jascha Sohl-Dickstein, Diederik P. Kingma, Abhishek Kumar, Stefano Ermon, and Ben Poole. Score-Based Generative Modeling through Stochastic Differential Equations. <https://arxiv.org/abs/2011.13456v2>, November 2020.
- Emanuel Todorov, Tom Erez, and Yuval Tassa. MuJoCo: A physics engine for model-based control. In *2012 IEEE/RSJ International Conference on Intelligent Robots and Systems*, pp. 5026–5033. IEEE, 2012. doi: 10.1109/IROS.2012.6386109.
- Unitree Robotics. Unitree rl lab: Reinforcement learning environments for unitree robots. https://github.com/unitreerobotics/unitree_rl_lab, 2025.
- Hado van Hasselt, Arthur Guez, and David Silver. Deep Reinforcement Learning with Double Q-learning, December 2015.
- Brent Yi, Hongsuk Choi, Himanshu Gaurav Singh, Xiaoyu Huang, Takara E. Truong, Carmelo Sferrazza, Yi Ma, Rocky Duan, Pieter Abbeel, Guanya Shi, Karen Liu, and Angjoo Kanazawa. Flow Policy Gradients for Robot Control. (arXiv:2602.02481), February 2026. doi: 10.48550/arXiv.2602.02481.
- Kevin Zakka, Baruch Tabanpour, Qiayuan Liao, Mustafa Haiderbhai, Samuel Holt, Jing Yuan Luo, Arthur Allshire, Erik Frey, Koushil Sreenath, Lueder A. Kahrs, Carlo Sferrazza, Yuval Tassa, and Pieter Abbeel. MuJoCo Playground: An open-source framework for GPU-accelerated robot learning and sim-to-real transfer., 2025.
- Yanjie Ze, Zixuan Chen, João Pedro Araújo, Zi-ang Cao, Xue Bin Peng, Jiajun Wu, and C. Karen Liu. TWIST: Teleoperated Whole-Body Imitation System. (arXiv:2505.02833), May 2025. doi: 10.48550/arXiv.2505.02833.
- Shuangfei Zhai, Ruixiang Zhang, Preetum Nakkiran, David Berthelot, Jiatao Gu, Huangjie Zheng, Tianrong Chen, Miguel Angel Bautista, Navdeep Jaitly, and Josh Susskind. Normalizing Flows are Capable Generative Models. (arXiv:2412.06329), June 2025. doi: 10.48550/arXiv.2412.06329.
- Yuanhang Zhang, Yifu Yuan, Prajwal Gurunath, Tairan He, Shayegan Omidshafiei, Ali-akbar Aghamohammadi, Marcell Vazquez-Chanlatte, Liam Pedersen, and Guanya Shi. FALCON: Learning Force-Adaptive Humanoid Loco-Manipulation. (arXiv:2505.06776), May 2025. doi: 10.48550/arXiv.2505.06776.

A APPENDIX

A.1 DETERMINATION OF VALUES IN TABLE 1

In this section, we explain how we choose the values for each algorithm presented in Table 1. We focus on explaining those that may cause confusion and omit the easy ones.

1. FastTD3 (Seo et al., 2025). In their paper, a critical modifications to the TD3 algorithm is to increase its batch size to a rather large value (roughly 32k). Combined with large off-policy replay buffer and massive environment numbers, the memory efficiency is sacrificed.
2. MaxEntDP (Dong et al., 2025). In their paper, to compute the log probability of diffusion policies (Eq. 21 in the original paper) and estimation of training target (Eq. 17 in the original paper), sampling-based approximation is employed. In high-dimensional space, the sampling number N and K is expected to be large and they use $N = 100$ and $K = 500$ as noted in their paper. In our setting, combined with large number of parallel environments (typical value 2048, 4096), this results in high consumption of memory.
3. GenPO (Ding et al., 2025). GenPO tries to compute the full Jacobian determinant without simplification used in Normalizing Flow and this brings much computation and memory burden. As noted in Conclusion and Limitation of their paper: ‘*Despite its excellent performance, GenPO faces the problem of relatively high computational and memory overhead to be resolved in the future.*’. And they used computing clusters with high memory and computation capacity as noted in their Appendix B.1.

The references: 1) FastTD3: (Seo et al., 2025); 2) Meow: (Chao et al., 2024) 3) MaxEntDP: (Dong et al., 2025); 4) GenPO: (Ding et al., 2025); 5) FPO: (McAllister et al., 2025)

A.2 ANALYSIS ON THE STABILITY OF TANH VS CLIP

In this section, we provide a theoretical analysis on why tanh may perform better than clip in mitigating the training instability.

Firstly, let’s recall we are maximizing

$$J(\theta) \approx \mathbb{E}[r(\theta)\tilde{A}(s, a)] \approx \mathbb{E}[\pi_\theta(a; s)] \approx \mathbb{E}\left[\exp\left(g(s_\theta(x))\right)\right] \text{ where } g \text{ is one of } \textit{identity function} \\ (g(x) = x), \textit{hard clip} (g(x; l) = \text{clip}(x, l)) \text{ and } \textit{tanh} (g(x; l) = l \tanh(x)) \text{ (} l \text{ would be omitted for brevity in below).}$$

If we analyze per-sample gradient of J against θ , we have:

$$G(x) = \nabla_\theta[\exp(g(s_\theta(x)))] = \exp(g(s))g'(s)\nabla_\theta s \quad (\text{S1})$$

and the per-sample gradient scale is determined by multiplication of 3 factors:

1. $\exp(g(s))$: an exponential scale over g
2. $g'(s)$: how much the signal of outer exponential passes through
3. $\nabla_\theta(s)$: the neural network’s sensitivity towards its parameters and are not influenced by the choice of g .

Identity Function. For $g(x) = x$, we have: $G(x) = \exp(s)\nabla(s)$ where $\exp(s)$ is unbounded and large s could cause exploding gradients, same as what we observed in Figure 2.

Hard Clip. For $g(x; l) = \text{clip}(x, l)$, we have: $G(x) = \exp(\text{clip}(s))g'(s)\nabla(s)$. While it helps bound the exponential value, there are 3 minor issues related to it: 1) When s is inside the range, the training signal is $\exp(s)$ which amplifies the gradient for larger s , creating a self-reinforcing push toward even larger values of s ; 2) When s is outside clipped range, the gradient is 0, i.e. no training signal is received from this sample. Hence the optimizer loses ability to move those samples back; 3) Together, many samples are driven toward the boundary $|s| = l$, once they cross they become gradient-dead under hard clipping, which can stall or bias training.

Tanh. We have $G(x) = \exp(\tanh(s))(1 - \tanh^2 s)\nabla s$. Besides bounded first term $\exp(\tanh(s))$, another good property is the second term $(1 - \tanh^2 s)$ is also smoothly decreasing as s increases. This helps optimizer to softly attenuate extreme values instead of zeroing them, so it avoids both exploding gradients and the “dead-zone” stalls caused by hard clipping.

A.3 ADDITIONAL EXPERIMENTS ON MUJOCO

In this section, we compare NFPO to various classic online RL methods on Mujoco (Todorov et al., 2012) environments, we use CleanRL (Huang et al., 2022) as the testbed. For SAC, TD3 and PPO, we use the original implementation and hyperparameters in CleanRL’s codebase. For NFPO, we just replace the policy parameterization from PPO and others remain the same. Note as SAC, TD3 are off-policy methods, *they generally obtain better sample efficiency* compared to PPO and NFPO.

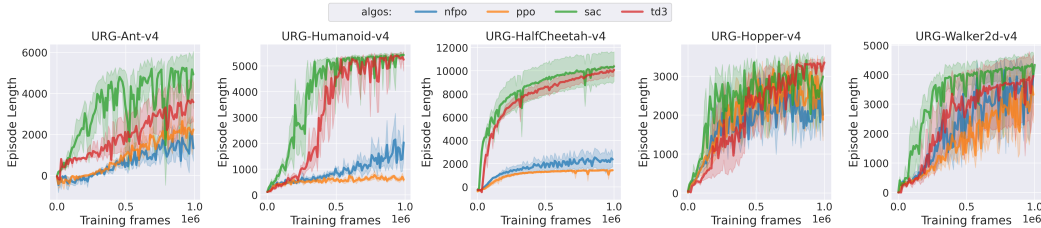


Figure S1: Performance of various online RL methods on Mujoco environments (5 seeds).

From the results, we could find NFPO could obtain similar performance compared to PPO on various simpler environments like Ant, HalfCheetah, Hopper and Walker2d. For complex environments like Humanoid, it achieves better performance compared to PPO, similar to what we’ve found in the main experiments.

A.4 ADDITIONAL ABLATION EXPERIMENTS OF NFPO

In this section, we further ablate on the *number of layers* and *hidden dimension size* of NFPO. The results are shown in Figure S2.

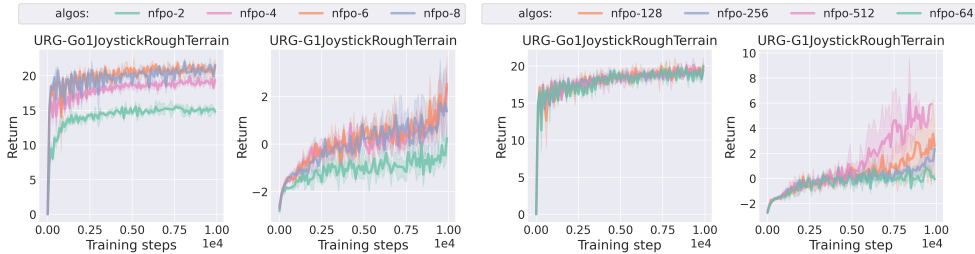


Figure S2: Performance of NFPO over various number of layers and hidden dimensions (5 seeds).

For number of layers, nfpo-2 achieves significant lower performance. This is because for odd-even-based masking we used, minimum 3 layers are required for expressiveness. For other number of layers (e.g., 4, 6 and 8), they generally obtain similar performance.

For hidden dimensions, they obtain quite similar results on simpler tasks like Go1JoystickRoughTerrain. For harder tasks like G1JoyStickRoughTerrain, NFPO-512 obtains best performance while NFPO-64 is the worst, and NFPO-128 and NFPO-256 obtain similar converged performance.

A.5 ADDITIONAL TUNING OF MEOW

We additionally perform hyperparameters tuning for Meow. For the hyperparameters, we mainly tuned polyak and entropy value (alpha) similar to their original paper (Chao et al., 2024)

and increased batch size to 10240 as recommended in Seo et al. (2025). Other hyperparameters are kept the same as in Meow’s original codebase. The results are in Figure S3 and the legend is meow-alpha-polyak (the tuned alpha values are $\{0.25, 0.1, 0.025\}$ and polyak values are $\{2.5e-4, 2.5e-2\}$). To facilitate the reproducibility, we also provide the source code we used for training Meow in Unitree RL Gym.

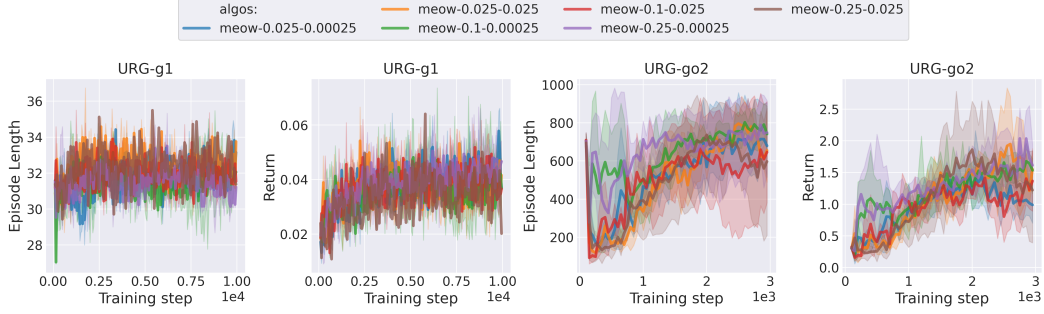


Figure S3: Performance of Meow over various tuned polyak and alpha. The experiments are in 3 seeds.

From the results, unfortunately, Meow generated no significant learning in these 2 environments. On URG-go2, its episode length is increased substantially, indicating it learns not to fall to ground to some extent but the episodic returns indicate that no meaningful locomotion or command following is learned. For URG-g1 which is more prone to fall, no significant learning in both episodic length and episodic return is observed.

A.6 STABILIZED DEPLOYMENT

Deployment on real-world whole-body-controlled humanoid robot is complex and could cause damages to the surrounding environments or assets. Hence, in our experiment, we supply the *mode* of base Gaussian distribution to reduce the stochastics and help stabilize the deployment. This is similar to the common practice in PPO where people use the *mean* ($\mu_\theta(s)$) as action in deployment (instead of sampling from $\mathcal{N}(\mu_\theta(s), \sigma_\theta(s))$ as in training).

This can also be seen as a similar case to what people do in temperature-based generation where high temperature favors more random generation while low temperature favors more optimal generation. For NFPO, temperature could be controlled in sampling $z \sim N(0, \tau I)$, for PPO, it’s in $a \sim N(\mu_\theta(s), \tau \sigma_\theta(s))$. In our experiments, for both PPO and NFPO, if we sample actions with a larger temperature (τ), both of them generate unstable behaviors. While using a low-temperature (a smaller τ that is not necessarily 0), both of them generate stable behaviors.

A.7 THE MODE OF NORMALIZING FLOWS

For RealNVP:

$$f_{\theta_j}(a)_{d_j} = a_{d_j} \quad (S2)$$

$$f_{\theta_j}(a)_{\setminus d_j} = a_{\setminus d_j} \odot \exp(s_{\theta_j}(a_{d_j})) + t_{\theta_j}(a_{d_j}) \quad (S3)$$

$$\text{we have } \log \pi(a) = \log q(f_\theta(a)) + \sum_j \log \left| \frac{df_{\theta_j}(a)}{da} \right| \quad (S4)$$

$$= \log q(f_\theta(a)) + \sum_j s_{\theta_j}(a_{d_j}) \quad (S5)$$

As it uses non-constant scale ($s_\theta(a)$), the mode in prior distribution ($\mathcal{N}(0, I)$) may not be the mode of data distributions. However, the $\log q(f_\theta(a))$ term still favors smaller latent and in practice we find sampling near the mode of prior distribution is sufficient to generate stable behavior as in Section A.6. This is also similar to what Kirichenko et al. (2020) finds that RealNVP tends to use t to reduce the effect of an increased s to get a smaller latent, as a way to meet the 2 objectives simultaneously.

In Chao et al. (2024), as they adopt NICE (Dinh et al., 2015) $(f_{\theta_j}(a)_{\setminus d_j} = a_{\setminus d_j} + t_{\theta_j}(a_{d_j}))$ which doesn't have varying scalar terms ($s_{\theta}(a) = 1$). Hence the mode in prior distribution is analytically the mode of data distribution.

A.8 PSEUDOCODE OF NFPO

In this section, we provide a pseudo code of NFPO in Algorithm 1.

Algorithm 1: Pseudo code of NFPO

Input: parallel environment e , initial network parameter θ , clip ratio ϵ

```

1 while training do
2    $B \leftarrow []$ 
3   for  $t = 1$  to  $T$  do
4      $z \sim q(z)$ 
5      $a \leftarrow f_{\theta}^{-1}(z; o)$ 
6      $\log a = \log(f_{\theta}(a)) + \sum_j \log \left| \frac{df_{\theta_j}(a; o)}{da} \right|$ 
7      $o', r, d \leftarrow \text{step}(e, a)$ 
8      $B \leftarrow \text{append}(B, (o, a, r, d, \log a, o'))$ 
9   end
10   $\tilde{A} \leftarrow \text{GAE}(B)$  // estimate advantage via GAE
11  for  $n = 1$  to  $N$  do
12     $bs \leftarrow \text{partition}(B)$  // partition large buffer  $B$  to smaller  $bs$ 
13    for  $m = 1$  to  $M$  do
14       $b \leftarrow bs[m]$ 
15       $agent \leftarrow \text{update}(agent, b)$ 
16    end
17  end
18 end
19 Function  $\text{update}(agent, b)$ 
20   /* the update of value function is not changed and omitted */
21    $o, \pi_{\text{old}}(a) \leftarrow b$ 
22    $r(\theta) \leftarrow \frac{\pi_{\theta}(a; o)}{\pi_{\text{old}}(a)}$ 
23    $L_{\theta} \leftarrow \nabla_{\theta} \frac{1}{|b|} \sum_b \left[ \min(r(\theta)\tilde{A}(s, a), \text{clip}(r(\theta), 1 - \epsilon, 1 + \epsilon)\tilde{A}(s, a)) \right]$ 
24    $agent \leftarrow \text{SGD}(agent, L_{\theta})$ 
25   return  $agent$ 

```

A.9 DETAILS OF HYPERPARAMETERS

We list the details of training hyperparameters in Table S1. For PPO and NFPO, most components and hyperparameters could be shared and major difference lies in the actor network parameterization which we have aligned in terms of parameter numbers.

A.10 DETAILS OF HARDWARE AND COMPUTATION EFFICIENCY

Most of our experiments run on a 16 CPU x 1 Nvidia A100-40G GPU except for Meow which needs more than 40G GPU memory and run on A100-80G.

Depending on specific training settings, the wall clock time of each experiment varies and we provide the wall clock time of PPO and NFPO on Unitree RL Gym's g1 environment in Table S2:

Table S1: Hyperparameter settings

Hyperparameter	Value	Remarks	
Shared	GAE λ	0.95	
	discount γ	0.99	
	value loss coefficient	1.0	
	grad clip	1.0	
	learning epoch	5	
	learning minibath	4	
	entropy loss coefficient	10^{-3}	only for PPO
	step length	24	
	desired KL divergence	10^{-2}	only for PPO adaptive
Unitree RL Gym	learning rate	10^{-3}	
	value network hidden dims	[32]	1 layer network with hidden dim 32
	PPO actor network hidden dimes	[96, 96, 64]	
	NFPO actor network hidden dimes	$4 \times [64]$	4 layers, each layer with 64 hidden dim
	number of environments	4096	
Mujoco Playground	learning rate	$5e^{-4}$	$3e^{-4}$ for manipulation tasks
	value network hidden dims	[512, 256, 128]	
	PPO actor network hidden dimes	[512, 256, 128]	
	NFPO actor network hidden dimes	$4 \times [256]$	
	number of environments	2048	

Table S2: Runtime of PPO and NFPO on Unitree Gym’s g1. Calculated using 10 seeds.

Algorithm	Runtime (s)	Runtime (h)	Ratio
PPO	13500.94 ± 628.29	3.75 ± 0.17	1
NFPO	16036.06 ± 795.74	4.45 ± 0.22	1.19